12

NUSC Technical Report 8785
9 October 1990

AD-A229 987

Alias-Free Smoothed Wigner Distribution Function for Discrete-Time Samples

Albert H. Nuttall
Surface ASW Directorate

DTIC
S ELECTE DEC 06 1990 D
E

Naval Underwater Systems Center
Newport, Rhode Island • New London, Connecticut

Approved for public release; distribution is unlimited.

PREFACE

This research was conducted under NUSC Project No. A70272, Subproject No. RR0000-N01, **Selected Statistical Problems in Acoustic Signal Processing**, Principal Investigator, Dr. Albert H. Nuttall (Code 304). This technical report was prepared with funds provided by the NUSC In-House Independent Research and Independent Exploratory Development Program, sponsored by the Office of the Chief of Naval Research.

The technical reviewer for this report was Dr. Kent N. Scarbrough (Code 304).

REVIEWED AND APPROVED: 9 OCTOBER 1990

Gerald M. Mayer

Gerald M. Mayer
Acting, Surface ASW Directorate

REPORT DOCUMENTATION PAGE

Form Approved
OMB No. 0704-0188

Public reporting burden for this collection of information is estimated to average 1 hour per response, including the time for reviewing instructions, searching existing data sources, gathering and maintaining the data needed, and completing and reviewing the collection of information. Send comments regarding this burden estimate or any other aspect of this collection of information, including suggestions for reducing this burden, to Washington Headquarters Services, Directorate for Information Operations and Reports, 1215 Jefferson Davis Highway, Suite 1204, Arlington, VA 22202-4302, and to the Office of Management and Budget, Paperwork Reduction Project (0704-0188), Washington, DC 20503

1. AGENCY USE ONLY *(Leave blank)*

2. REPORT DATE
9 October 1990

3. REPORT TYPE AND DATES COVERED
Progress

4. TITLE AND SUBTITLE
Alias-Free Smoothed Wigner Distribution Function for Discrete-Time Samples

5. FUNDING NUMBERS
PE 61152N

6. AUTHOR(S)
Albert H. Nuttall

7. PERFORMING ORGANIZATION NAME(S) AND ADDRESS(ES)
Naval Underwater Systems Center
New London Laboratory
New London, CT 06320

8. PERFORMING ORGANIZATION REPORT NUMBER
TR 8785

9. SPONSORING/MONITORING AGENCY NAME(S) AND ADDRESS(ES)
Chief of Naval Research
Office of the Chief of Naval Research
Arlington, VA 22217-5000

10. SPONSORING/MONITORING AGENCY REPORT NUMBER

11. SUPPLEMENTARY NOTES

12a. DISTRIBUTION/AVAILABILITY STATEMENT
Approved for public release; distribution is unlimited.

12b. DISTRIBUTION CODE

13. ABSTRACT *(Maximum 200 words)*

An alias-free Wigner distribution function (WDF), for a time waveform s(t) limited to total frequency extent F, is available if the time sampling increment Δ is less than 1/F. Furthermore, the WDF can be efficiently numerically evaluated via fast Fourier transform (FFT) procedures if the FFT size N is greater than $2T/\Delta$, where T is the effective duration of s(t).

However, in order to suppress the undesired inherent oscillating interference terms in the WDF, it is necessary to smooth the WDF, or equivalently, weight the complex ambiguity function. This smoothing operation cannot be accomplished without a penalty in terms of sampling increment Δ and FFT size N. In particular, if the smearings in the time and frequency domains of the WDF are 2/B and 2/D, respectively, the new tighter requirements are

14. SUBJECT TERMS
Aliasing
Ambiguity Function
Discrete Time
FFT Size
Smoothing
Spectral Correlation
Temporal Correlation
Tilted Weighting
Time-Frequency Distribution
Time Increment

15. NUMBER OF PAGES
34

16. PRICE CODE

17. SECURITY CLASSIFICATION OF REPORT	18. SECURITY CLASSIFICATION OF THIS PAGE	19. SECURITY CLASSIFICATION OF ABSTRACT	20. LIMITATION OF ABSTRACT
UNCLASSIFIED	UNCLASSIFIED	UNCLASSIFIED	SAR

13. ABSTRACT (Cont'd)

$$\Delta < \left(F + \frac{2}{D}\right)^{-1} , \quad N > \frac{2T}{\Delta} + \frac{4}{B\Delta} .$$

The impact of these more stringent bounds, which depends on the particular waveform s(t) of interest and the degree of smoothing utilized, must be anticipated and investigated for each case; if either bound is violated, an aliased smoothed WDF will result.

14. SUBJECT TERMS (Cont'd)

Weighting
Wigner Distribution
Windowing

Accession For	
NTIS GRA&I	X
DTIC TAB	☐
Unannounced	☐
Justification	
By	
Distribution/	
Availability Codes	
Dist	Avail and/or Special
A-1	

DTIC COPY

TABLE OF CONTENTS

LIST OF ILLUSTRATIONS

LIST OF ABBREVIATIONS

FFT	fast Fourier transform
WDF	Wigner distribution function
CAF	complex ambiguity function
TCF	temporal correlation function
SCF	spectral correlation function
TFR	time-frequency representation
GTFR	generalized time-frequency representation

LIST OF SYMBOLS

t	time, (1)
f	frequency, (1)
$s(t)$	waveform of interest, (1)
$S(f)$	spectrum of $s(t)$, (1)
T	total time extent of $s(t)$, (2)
F	total frequency extent of $S(f)$, (3)
τ	time delay or separation, (4)
ν	frequency shift or separation, (5)
$R(t,\tau)$	temporal correlation function, (4)
$\Phi(\nu,f)$	spectral correlation function, (5)
$W(t,f)$	Wigner distribution function, (6)
$\chi(\nu,\tau)$	complex ambiguity function, (7)
$\tilde{v}(\nu,\tau)$	weighting or kernel, (8)
$\tilde{V}(\nu,f)$	bispectral function, (9)
$v(t,\tau)$	bitemporal function, (10)
$V(t,f)$	smoothing function, (11)
B	$1/B$ is positive extent of $V(t,f)$ in t, figures 2 and 4
D	$1/D$ is positive extent of $V(t,f)$ in f, figures 2 and 4
$\chi(\nu,\tau)$	modified complex ambiguity function, (16)
$\Phi(\nu,f)$	modified spectral correlation function, (17)
$R(t,\tau)$	modified temporal correlation function, (18)
$W(t,f)$	modified Wigner distribution function, (19)
$\oplus$	convolution, under (19)
r	tilt parameter, (23) and figure 4
q	$(1-r^2)^{1/2}$, (24)

A_{tf}	effective area of $V(t,f)$, figure 4
$A_{\nu\tau}$	effective area of $\tilde{v}(\nu,\tau)$, figure 4
σ	parameter of Choi-Williams kernel, (25)
Δ	time increment in sampling $s(t)$, (31)
$\bar{S}(f)$	spectrum calculated from samples $\{s(k\Delta)\}$, (31)
N	FFT size, (33)
Δ_f	frequency increment, (33)
sub a	approximation, (34), (42), (48)
δ_b	infinite impulse train of period b, (35)
Δ_ν	increment in ν, (39)
Δ_τ	increment in τ, (40)
Δ_t	increment in t, (52)

ALIAS-FREE SMOOTHED WIGNER DISTRIBUTION FUNCTION FOR DISCRETE-TIME SAMPLES

INTRODUCTION

The utility of the Wigner distribution function (WDF) for detailed time-frequency analysis of waveforms has been summarized very well in a recent article by Cohen [1]; this material will be assumed to be known by the reader. As for actual numerical calculation, the problem of obtaining an alias-free WDF and complex ambiguity function (CAF), from discrete-time samples, was solved in a recent report by Nuttall [2]. Specifically, an upper bound on the time sampling increment and a lower bound on the fast Fourier transform (FFT) size were determined that allowed for evaluation of the original continuous WDF and CAF at a discrete set of points with sufficient detail and coverage to avoid any significant loss of information. Furthermore, a detailed prescription for the required data processing of the available discrete-time samples, in terms of FFTs, was given.

However, the presence of large oscillating interference terms, which are inherent to the WDF, requires that some smoothed version of the WDF be made available from discrete data. This problem was addressed recently by Harms [3], and a procedure was delineated for its realization in terms of FFTs. However, the additional data processing required for the smoothed WDF cannot be realized without some extra effort or penalty; in fact, new more stringent bounds on the sampling increment and FFT sizes must be met in order to retain the alias-free character of the resultant smoothed WDF. These bounds were derived by Nuttall and furnished to Harms who listed them in [3; section 4 (see his reference 11)].

In this current report, we will present the detailed derivations that lead to these bounds. In the process, interpretations of the smoothed temporal correlation function (TCF) and smoothed spectral correlation function (SCF) are required and furnished. Allowance for a very general form of ambiguity weighting (multiplication) or Wigner smoothing (convolution), including tilts in the appropriate time-frequency planes, is made and accounted for. The specific data processing and FFT operations are presented in complete detail.

CONTINUOUS TIME-FREQUENCY REPRESENTATIONS

In this section, waveform $s(t)$ is considered to be available for continuous time t. We will point out some basic properties of the various time-frequency representations (TFRs) of the waveform, which will be required later when we address the discrete-time case; some of this material was given in [2; especially appendix A].

WAVEFORM CHARACTERISTICS

Complex waveform $s(t)$ has voltage density spectrum

$$S(f) = \int dt \exp(-i2\pi ft)\, s(t) \,, \tag{1}$$

where f is cyclic frequency and integrals without limits are conducted over the range of nonzero integrand. It will be presumed that the waveform is essentially time limited and frequency limited; that is,

$$|s(t)| \simeq 0 \quad \text{for } |t| > T/2 \tag{2}$$

and

$$|S(f)| \simeq 0 \quad \text{for } |f| > F/2 \,. \tag{3}$$

Thus, the total time extent of $s(t)$ is T seconds while the total frequency extent of $S(f)$ is F Hertz. The effective extent of $s(t)$, say where $|s(t)|$ is within $1/e$ of its peak, is smaller than T; similarly, the effective extent of $S(f)$ is smaller than F.

This distinction between the essential (total) extent and the effective extent is kept below. The time-bandwidth product TF must be larger than 1 and can be much larger than 1 for some waveforms with detailed amplitude- and/or frequency-modulation.

The fact that s(t) is centered at t = 0 results in no loss of generality because we can delay or advance a given waveform to this location. Similarly, a centered spectrum S(f) is easily achieved by frequency shifting. We allow for complex s(t), thereby accommodating analytic or complex envelope waveforms.

TIME-FREQUENCY REPRESENTATIONS

The temporal correlation function (TCF) of s(t) is defined as

$$R(t,\tau) = s(t+\tfrac{1}{2}\tau)\, s^{*}(t-\tfrac{1}{2}\tau) \ . \tag{4}$$

Reference to (2) immediately reveals that $R(t,\tau)$ is essentially confined to $|t| < T/2$, $|\tau| < T$. The quantity τ is the time delay or separation variable.

The spectral correlation function (SCF) is the double Fourier transform of $R(t,\tau)$ and is given by

$$\Phi(\nu,f) = \iint dt\, d\tau\, \exp(-i2\pi\nu t - i2\pi f\tau)\, R(t,\tau) =$$

$$= S(f+\tfrac{1}{2}\nu)\, S^{*}(f-\tfrac{1}{2}\nu) \ . \tag{5}$$

Use of (3) then demonstrates that $\Phi(\nu,f)$ is essentially limited to $|\nu| < F$, $|f| < F/2$. The quantity ν is the frequency shift or separation variable.

The Wigner distribution function (WDF) is then given by either of the following transforms

$$W(t,f) = \int d\tau \; \exp(-i2\pi f\tau) \; R(t,\tau) = \tag{6a}$$

$$= \int d\nu \; \exp(+i2\pi\nu t) \; \Phi(\nu,f) \; . \tag{6b}$$

From (6a), we can conclude that $W(t,f)$ is confined to $|t| < T/2$, while from (6b), the frequency extent is essentially $|f| < F/2$.

Finally, the complex ambiguity function (CAF) is available from either of the following transforms

$$\chi(\nu,\tau) = \int dt \; \exp(-i2\pi\nu t) \; R(t,\tau) = \tag{7a}$$

$$= \int df \; \exp(+i2\pi f\tau) \; \Phi(\nu,f) \; . \tag{7b}$$

Therefore, the region of essential contribution of $\chi(\nu,\tau)$ is $|\nu| < F$, $|\tau| < T$, from (7b) and (7a), respectively.

The extents of all four of these two-dimensional time-frequency representations are summarized in figure 1. In fact, for Gaussian waveform $s(t) = a \exp(-\frac{1}{2}t^2/\sigma^2)$, the choices $T = 4\sigma$ and $F = 2/(\pi\sigma)$, for example, give these exact results in figure 1, at the $\exp(-4) = .018$ level. Horizontal movement in this figure is accomplished by means of a Fourier transform between variables t and ν; vertical movement utilizes a Fourier transform relationship between τ and f. Relations (6) and (7), along with their inverse Fourier transforms, constitute the totality of these one-dimensional transforms.

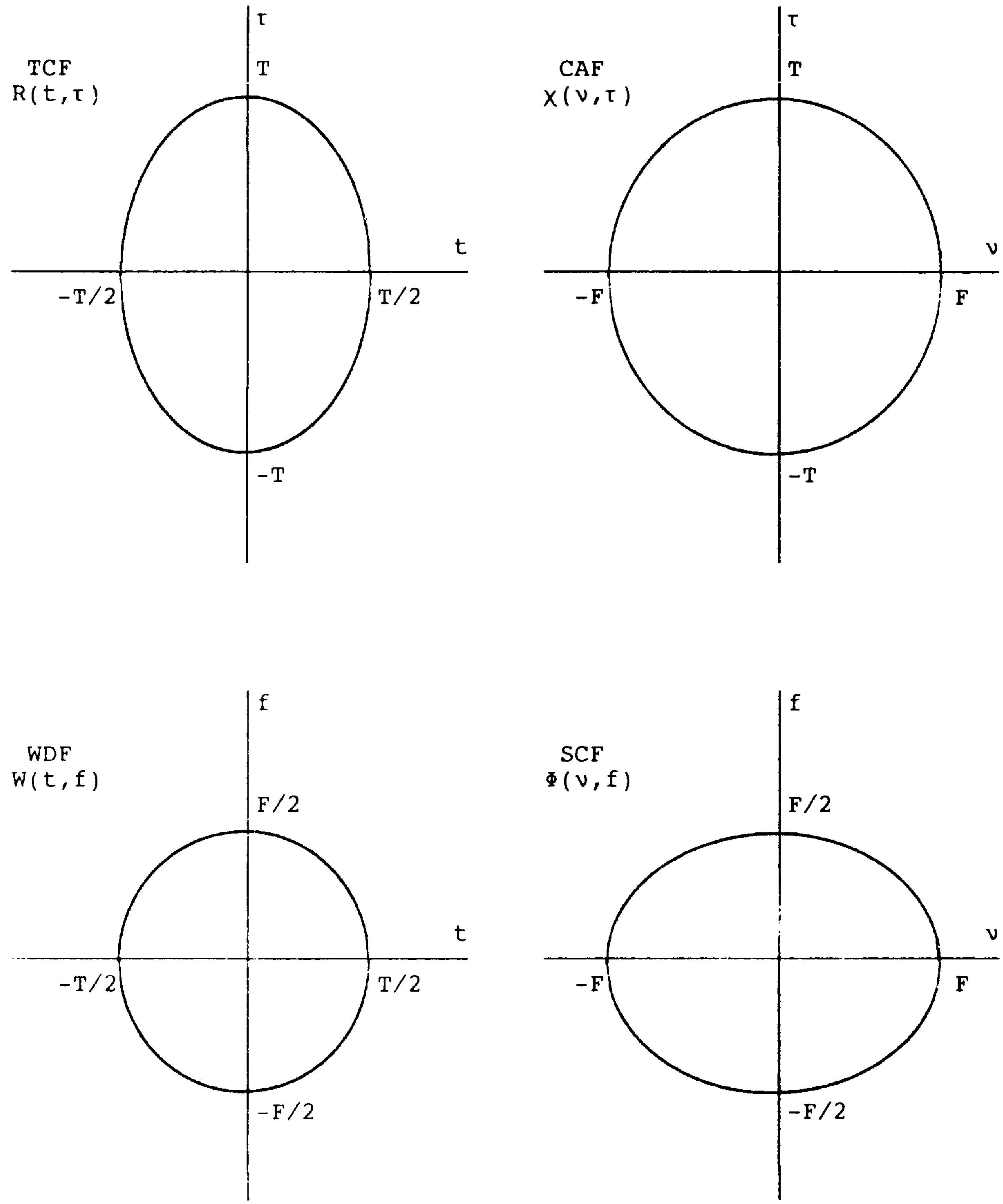

Figure 1. Extents of the Time-Frequency Representations

GENERALIZED TIME-FREQUENCY REPRESENTATIONS

Since there are four two-dimensional domains of interest in the TFRs depicted in figure 1, it is necessary to consider the effects of weighting and smoothing in all of them.

TWO-DIMENSIONAL SMOOTHING OPERATIONS

Consider ν,τ weighting (or kernel) $\tilde{v}(\nu,\tau)$ applied multiplicatively to CAF $\chi(\nu,\tau)$ to yield modified (weighted) CAF

$$X(\nu,\tau) = \chi(\nu,\tau)\ \tilde{v}(\nu,\tau) \ . \tag{8}$$

The three equivalent descriptors to weighting $\tilde{v}(\nu,\tau)$, in the remaining domains, are given by Fourier transform relations

$$\tilde{V}(\nu,f) = \int d\tau\ \exp(-i2\pi f\tau)\ \tilde{v}(\nu,\tau) \ , \tag{9}$$

$$v(t,\tau) = \int d\nu\ \exp(+i2\pi\nu t)\ \tilde{v}(\nu,\tau) \ , \tag{10}$$

$$\begin{aligned} V(t,f) &= \int d\tau\ \exp(-i2\pi f\tau)\ v(t,\tau) = \\ &= \int d\nu\ \exp(+i2\pi\nu t)\ \tilde{V}(\nu,f) = \\ &= \iint d\nu\ d\tau\ \exp(+i2\pi\nu t - i2\pi f\tau)\ \tilde{v}(\nu,\tau) \ . \end{aligned} \tag{11}$$

The last function, $V(t,f)$ in (11), will be called the smoothing function, for reasons to be seen below. The notational convention adopted here is that a Fourier transform from t to ν is indicated by a tilda, while a Fourier transform from τ to f is indicated by a capital.

GAUSSIAN EXAMPLE

Probably the simplest example of a unimodal two-dimensional smoothing operation in all four domains is furnished by the following Gaussian example, where B and D are arbitrary:

$$\tilde{v}(\nu,\tau) = \exp(-\pi\nu^2/B^2-\pi\tau^2/D^2) \quad , \tag{12}$$

$$\tilde{V}(\nu,f) = D \exp(-\pi\nu^2/B^2-\pi D^2 f^2) \quad , \tag{13}$$

$$v(t,\tau) = B \exp(-\pi B^2 t^2-\pi\tau^2/D^2) \quad , \tag{14}$$

$$V(t,f) = BD \exp(-\pi B^2 t^2-\pi D^2 f^2) \quad . \tag{15}$$

The effective areas of these four two-dimensional functions, at the 1/e contour level relative to each peak, are BD, B/D, D/B, and 1/(BD), respectively. It is seen from (12) that B and D are the essential (positive) extents of weighting $\tilde{v}(\nu,\tau)$ in the ν and τ directions, respectively. That is, $\tilde{v}(B,0) = \tilde{v}(0,D) = \exp(-\pi) = .043 \ll 1 = \tilde{v}(0,0)$. Similarly, from (15), 1/B and 1/D are the essential (positive) extents of smoothing function V(t,f) in the t and f dimensions, respectively. These properties are illustrated in figure 2, where each contour depicted is at level $\exp(-\pi) = .043$, relative to its peak. Shortly, we will generalize this smoothing function example to allow for tilts in the ν,τ and t,f planes, thereby enabling better smoothing capability to be applied to the WDF, without loss of significant information.

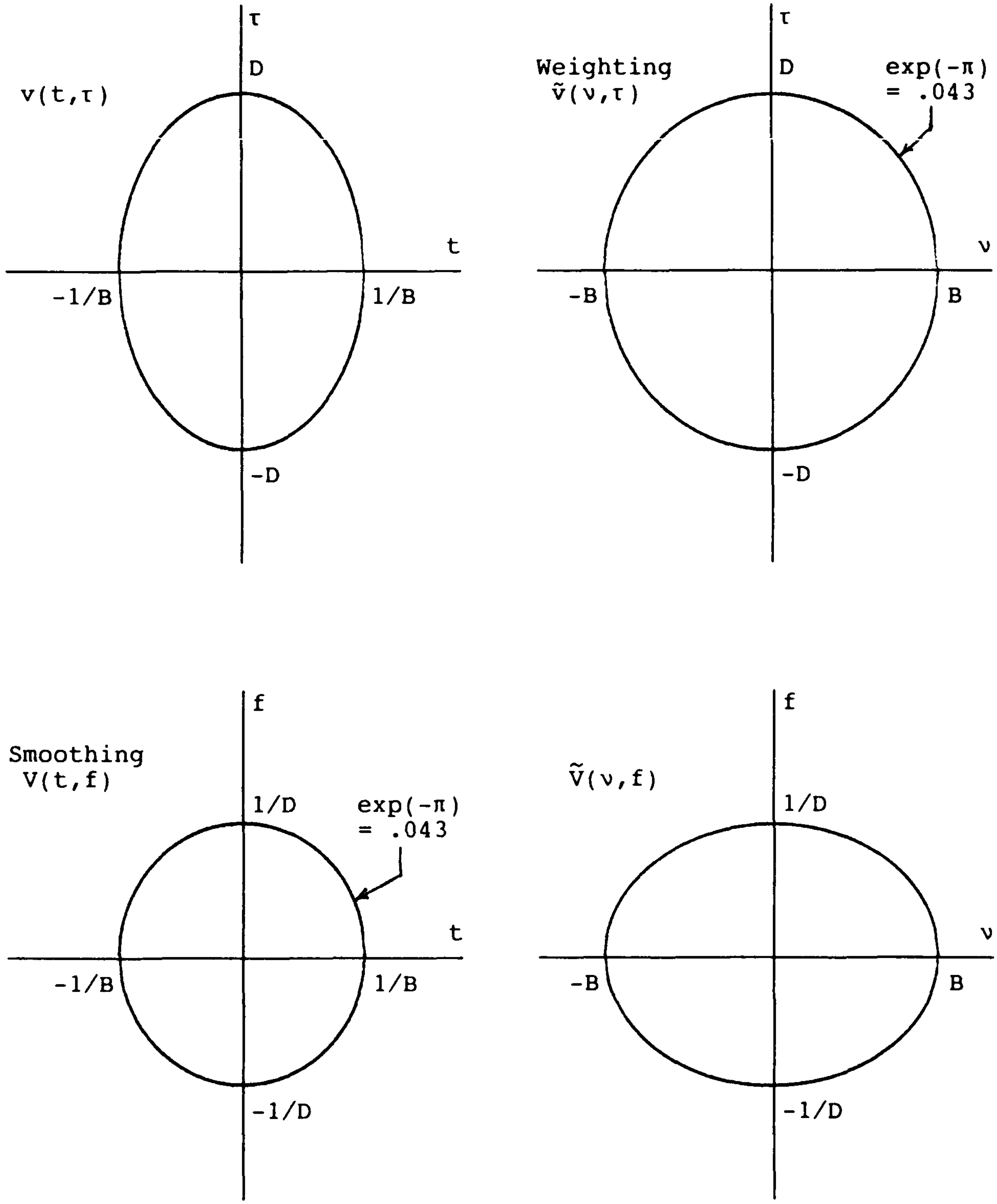

Figure 2. Two-Dimensional Smoothing Functions

MODIFIED TIME-FREQUENCY REPRESENTATIONS

The effects of each of the general smoothing functions in (8) - (11) on the four two-dimensional TFRs (4) - (7) of the previous section are now investigated; see also [4; appendix F]. The resultant generalized time-frequency representations (GTFRs) are indicated on the left-hand sides by bold type:

$$\boldsymbol{\chi}(\nu,\tau) \equiv \chi(\nu,\tau)\ \tilde{v}(\nu,\tau)\ , \tag{16}$$

$$\boldsymbol{\Phi}(\nu,f) \equiv \int d\tau\ \exp(-i2\pi f\tau)\ \boldsymbol{\chi}(\nu,\tau) = \Phi(\nu,f) \overset{f}{\oplus} \tilde{V}(\nu,f)\ , \tag{17}$$

$$\mathbf{R}(t,\tau) \equiv \int d\nu\ \exp(+i2\pi\nu t)\ \boldsymbol{\chi}(\nu,\tau) = R(t,\tau) \overset{t}{\oplus} v(t,\tau)\ , \tag{18}$$

$$\mathbf{W}(t,f) \equiv \int d\tau\ \exp(-i2\pi f\tau)\ \mathbf{R}(t,\tau) = W(t,f) \overset{tf}{\oplus} V(t,f)\ . \tag{19}$$

Here, $\overset{x}{\oplus}$ denotes convolution on x, with all other variables held fixed; thus, for example, (17) is $\int df'\ \Phi(\nu,f-f')\ \tilde{V}(\nu,f')$.

The interpretations of (16) - (19) are as follows: the CAF is simply multiplied by weighting $\tilde{v}(\nu,\tau)$; the SCF is smeared in frequency f according to $\tilde{V}(\nu,f)$; the TCF is smeared in time t according to $v(t,\tau)$; and the WDF is smeared in both t and f according to smoothing function $V(t,f)$. It is this latter two-dimensional smoothing (convolution) operation in t,f space that suppresses or eliminates the undesired oscillating components that are present in the original WDF, at the expense, of course, of spreading out localized energy components of the waveform.

The extents of the GTFRs are sketched in figure 3; these results are based upon (16) - (19), in combination with figures 1 and 2. Because $\chi(\nu,\tau)$ is the result of multiplication (16), its extents in ν,τ are the minima of the two contributing functions. On the other hand, the f extent of $\Phi(\nu,f)$ is increased by 1/D, which is the positive extent of $\tilde{V}(\nu,f)$ in f. Similarly, the t extent of $R(t,\tau)$ is lengthened by 1/B, owing to the smoothing action of $v(t,\tau)$. In both of these latter cases, the length of the untransformed variable (ν for $\Phi(\nu,f)$ and τ for $R(t,\tau)$) is unchanged. Finally, $W(t,f)$ is lengthened by 1/B and 1/D in the t and f dimensions, respectively, owing to the double convolution with smoothing function $V(t,f)$.

Since the smoothing function $V(t,f)$ in figure 2 has essentially reached zero by the time $|t| = 1/B$ and $|f| = 1/D$, the <u>effective</u> extents in t and f are approximately $|t| < 1/(2B)$ and $|f| < 1/(2D)$. That is, $V(t,f)$ is approximately 1/B by 1/D wide in the t,f plane, for an effective area of 1/(BD); see the line under (15). If this area 1/(BD) is .5 or greater, then we can expect that smoothed WDF $W(t,f)$ will be everywhere positive [4; (F-7) - (F-19)].

On the other hand, if effective area 1/(BD) is significantly less than .5, then smoothing function $V(t,f)$ is rather impulsive-like and little averaging will occur as a result of double convolution (19). Thus, it appears that BD, at least for the simple Gaussian example in (12) - (15) and figure 2, should be chosen of the order of 3 to 4. Then, the effective area of weighting $\tilde{v}(\nu,\tau)$ in (12) and figure 2 is BD, which is of the

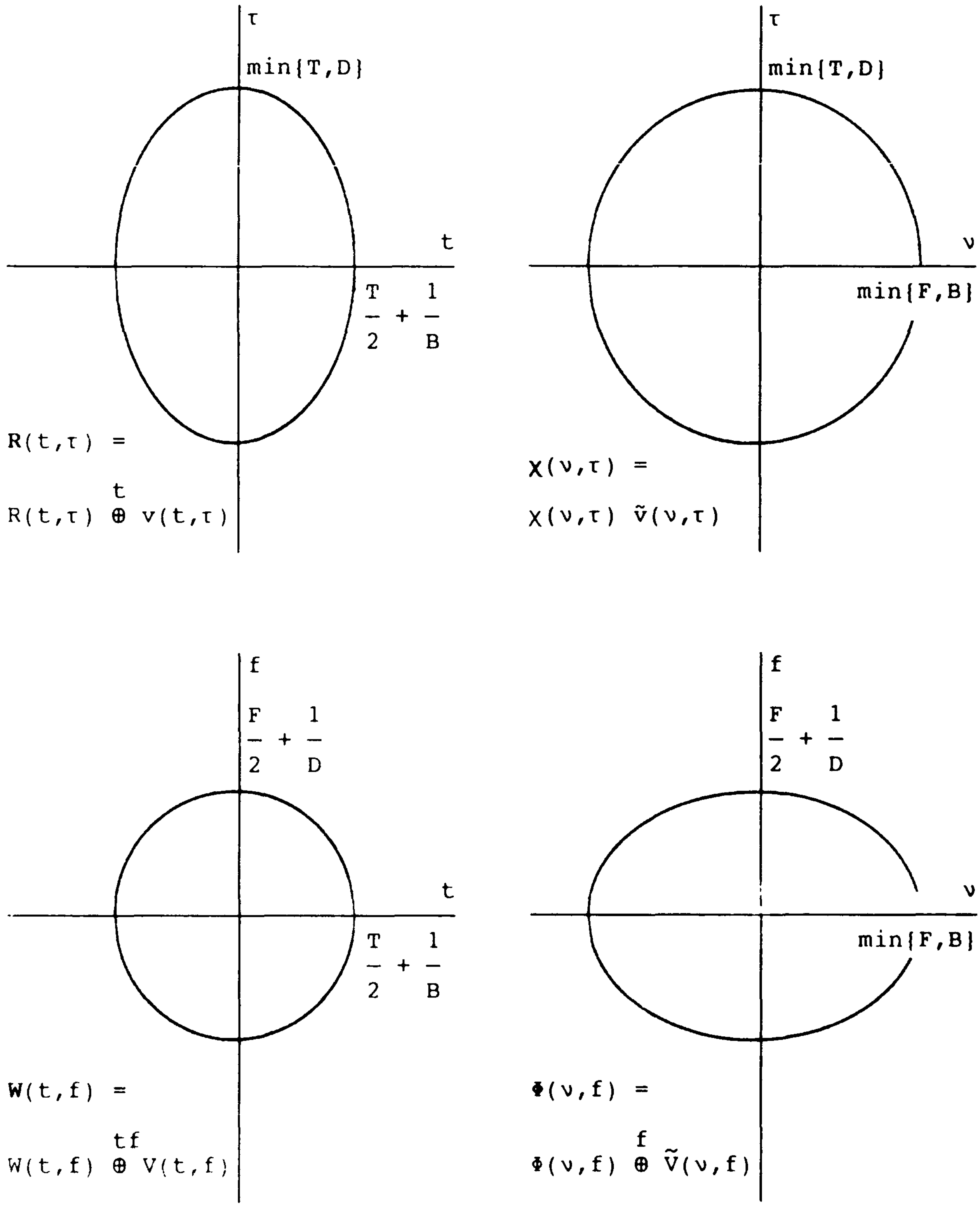

Figure 3. Generalized Time-Frequency Representations

order of 3 to 4. This area is significantly smaller than the effective extent of CAF $\chi(\nu,\tau)$ in figure 1, which covers an area of the order of FT, which is generally much larger than 1. Therefore, we can anticipate significant modifications in the weighted CAF $\boldsymbol{\chi}(\nu,\tau)$, and, hence, in the smoothed WDF $\mathbf{W}(t,f)$, in the majority of the t,f plane. Except to say that we expect that B < F and D < T, there is little quantitative connection between these parameters, in general.

TILTED GAUSSIAN EXAMPLE

When waveform s(t) contains some linear frequency modulation, the simple Gaussian smoothing functions in (12) - (15) and figure 2 are inadequate. The CAF and WDF of s(t) have contours in their respective planes that are similar to tilted ellipses; see, for example, [4; pages 35 - 39]. It is then necessary to realize a weighting function $\tilde{v}(\nu,\tau)$ and a smoothing function V(t,f), which also have the capability of moving their contours to approximately match those of typical CAFs and WDFs.

A very useful set of smoothing functions is furnished by the tilted Gaussian mountain, with B and D arbitrary [4; appendices F and D]:

$$\tilde{v}(\nu,\tau) = \exp\left[-\pi\left(\frac{\nu^2}{B^2} + \frac{\tau^2}{D^2} + 2r\,\frac{\nu}{B}\,\frac{\tau}{D}\right)\right] , \tag{20}$$

$$\tilde{V}(\nu,f) = D\,\exp\left[-\pi\left(\left(1-r^2\right)\frac{\nu^2}{B^2} + D^2 f^2 - i2r\,\frac{\nu}{B}\,Df\right)\right] , \tag{21}$$

$$v(t,\tau) = B \exp\left[-\pi\left(B^2t^2 + \left(1-r^2\right)\frac{\tau^2}{D^2} + i2r\ Bt\ \frac{\tau}{D}\right)\right] , \qquad (22)$$

$$V(t,f) = \frac{BD}{\left(1-r^2\right)^{1/2}} \exp\left[-\frac{\pi}{1-r^2}\left(B^2t^2 + D^2f^2 + 2r\ Bt\ Df\right)\right] . \qquad (23)$$

For $r = 0$, these reduce to (12) - (15). Plots of weighting function $\tilde{v}(\nu,\tau)$ and smoothing function $V(t,f)$ are displayed in figure 4; the contours drawn are at the $\exp(-\pi) = .043$ level relative to the peak value of each function. Dimensionless tilt parameter r is limited to $|r| < 1$; also, we define $q = (1-r^2)^{1/2}$.

The smoothing function $V(t,f)$ again has essential extent $2/B$ by $2/D$ in the t,f plane; that is, $V(t,f)$ is substantially zero for $|t| > 1/B$ or $|f| > 1/D$. However, the effective area A_{tf} (inside the $1/e$ relative contour level) of $V(t,f)$ is now $q/(BD)$, which can be considerably less than $1/(BD)$ for $|r|$ near 1, that is, when $q << 1$. Weighting function $\tilde{v}(\nu,\tau)$ now has essential extent $2B/q$ by $2D/q$ in the ν,τ plane; its effective area $A_{\nu\tau}$ is BD/q, which is the reciprocal of that for smoothing function $V(t,f)$: $A_{\nu\tau} = 1/A_{tf}$. Values of A_{tf} of the order of 1/3 to 1/4 are desired for smoothing purposes; then, $A_{\nu\tau} \sim 3$ to 4.

Although effective area A_{tf} can be considerably less than $1/(BD)$, the smearing caused by double convolution (19) still leads to a smoothed WDF $\mathbf{W}(t,f)$ which occupies the same region indicated in figure 3. The extents of the four GTFRs are exactly the same as figure 3, except that the limits on ν and τ are now

$$\min\{F,B/q\} \quad \text{and} \quad \min\{T,D/q\}, \text{ respectively;} \quad q = (1-r^2)^{1/2} . \qquad (24)$$

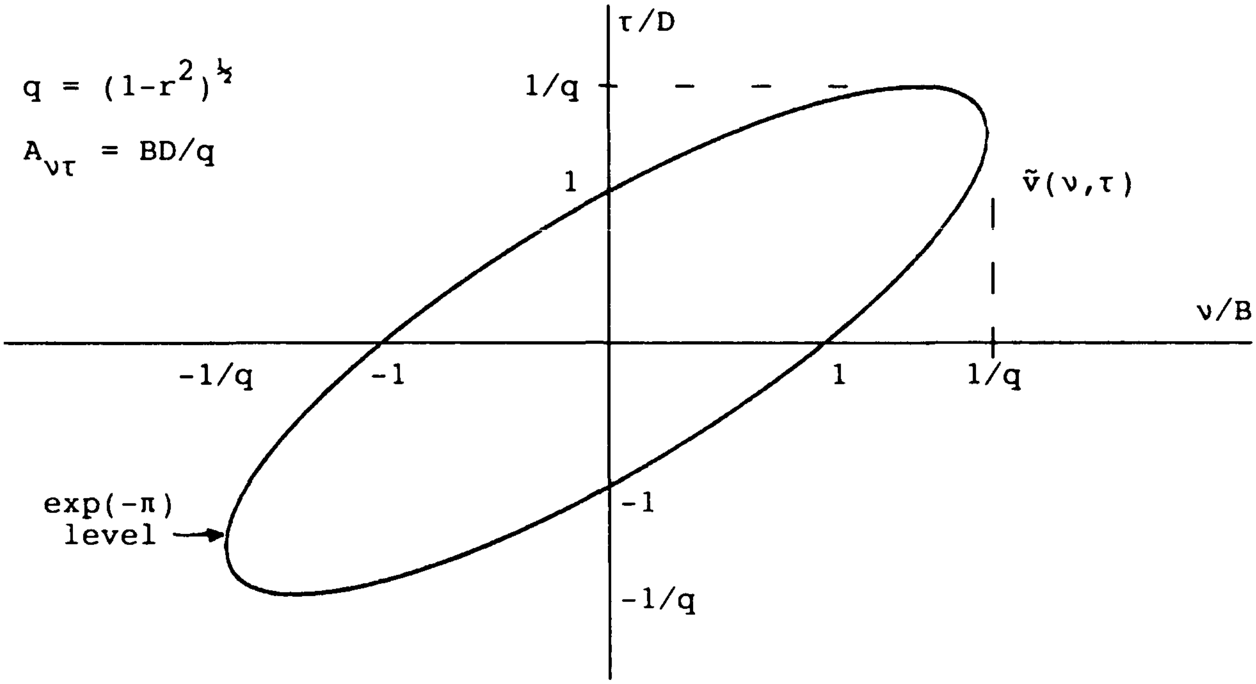

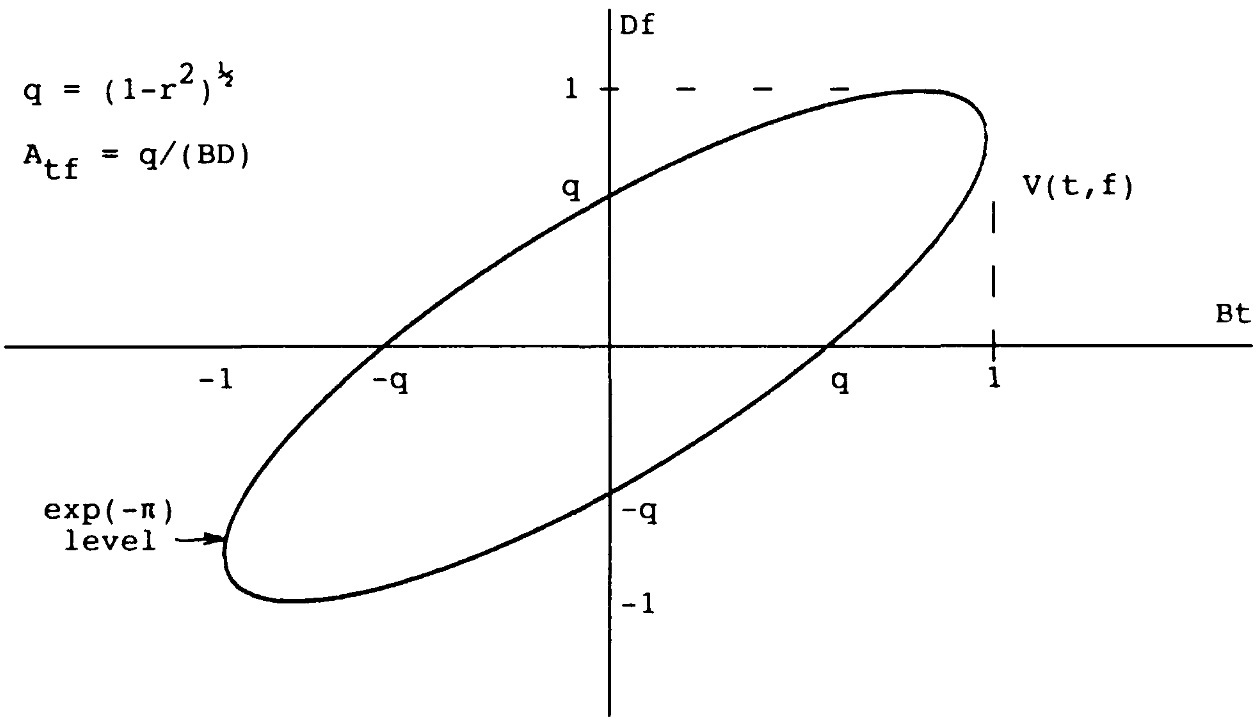

Figure 4. Tilted Smoothing Functions

CHOI-WILLIAMS KERNEL

Another example of the smoothing operations in (8) - (11) is furnished by [5]:

$$\tilde{v}(\nu,\tau) = \exp(-\nu^2\tau^2/\sigma^2) \,, \quad \sigma > 0 \,, \tag{25}$$

$$v(t,\tau) = \begin{Bmatrix} \pi^{\frac{1}{2}}\sigma/|\tau| \; \exp(-\pi^2\sigma^2 t^2/\tau^2) & \text{for } \tau \neq 0 \\ \delta(t) & \text{for } \tau = 0 \end{Bmatrix} , \tag{26}$$

$$\tilde{V}(\nu,f) = \begin{Bmatrix} \pi^{\frac{1}{2}}\sigma/|\nu| \; \exp(-\pi^2\sigma^2 f^2/\nu^2) & \text{for } \nu \neq 0 \\ \delta(f) & \text{for } \nu = 0 \end{Bmatrix} , \tag{27}$$

$$V(t,f) = 2\pi^{\frac{1}{2}}\sigma \int_{0+}^{+\infty} \frac{d\nu}{\nu} \cos(2\pi\nu t) \exp(-\pi^2\sigma^2 f^2/\nu^2) = \tag{28a}$$

$$= 2\pi^{\frac{1}{2}}\sigma \int_{0+}^{+\infty} \frac{d\tau}{\tau} \cos(2\pi f\tau) \exp(-\pi^2\sigma^2 t^2/\tau^2) \,, \tag{28b}$$

provided that $t \neq 0$ and $f \neq 0$. Integral (28a) is convergent at $\nu = 0+$ only if $f \neq 0$ and is convergent at $\nu = +\infty$ only if $t \neq 0$. Similarly, (28b) converges at $\tau = 0+$ only if $t \neq 0$ and converges at $\tau = +\infty$ only if $f \neq 0$. Also, (28) yields $V(0,f) = \infty$ for all finite f, and $V(t,0) = \infty$ for all finite t. This smoothing function $V(t,f)$ in (28) has an integrable singularity all along both coordinate axes since $\tilde{v}(0,0) = \iint dt\,df\; V(t,f) = 1$ is finite. Probably $V(t,f)$ has a logarithmic singularity as $tf \to 0$. Letting $\tau = |t|x$ in (28b), $V(t,f)$ is seen to be a function only of $|tf|$.

Because of these singularities, the actual numerical calculation of the GTFR $\mathbf{W}(t,f)$, by means of double convolution (19), appears very unattractive; rather, the Fourier transform in (19) is the recommended procedure. The delta functions in the bottom lines of (26) and (27) mean that

$$R(t,0) = R(t,0) \quad \text{and} \quad \Phi(0,f) = \Phi(0,f) \ . \tag{29}$$

These results follow directly from (18) and (17), respectively. Therefore, when computing GTFR $\mathbf{R}(t,\tau)$ by means of the Fourier transform in (18), the slice for $\tau = 0$ need not be done at all, but rather (29) should be employed. That is,

$$\mathbf{R}(t,\tau) = \left\{ \begin{array}{lr} \int d\nu \, \exp(i2\pi\nu t) \, \chi(\nu,\tau) \, \exp(-\nu^2\tau^2/\sigma^2) & \text{for } \tau \neq 0 \\ R(t,0) = |s(t)|^2 & \text{for } \tau = 0 \end{array} \right\} . \tag{30}$$

Finally, GTFR $\mathbf{W}(t,f)$ is obtained by Fourier transform (19). Numerous other possibilities for kernel $\tilde{v}(\nu,\tau)$ are listed in [1].

PRODUCT KERNELS

The weighting in (25) is an example of a product kernel, that is, the weighting takes the form

$$\tilde{v}(\nu,\tau) = g(\nu\tau) \ , \quad g(0) = 1 \ . \tag{30a}$$

In order that smoothing function $V(t,f)$ be real for all t,f, it is necessary that $\tilde{v}^\star(-\nu,-\tau) = \tilde{v}(\nu,\tau)$ for all ν,τ, which in turn requires that $g(x)$ be real for all arguments x. Now define

$$G(y) = \int dx \, \exp(-i2\pi xy) \, g(x) \; . \tag{30b}$$

Then $G(-y) = G^*(y)$ for all y.

With the help of these functions and properties, we find that the rest of the two-dimensional smoothing functions are given by

$$\tilde{V}(\nu,f) = \left\{ \begin{array}{ll} \frac{1}{|\nu|} G\left(\frac{f}{\nu}\right) & \text{for } \nu \neq 0 \\ \delta(f) & \text{for } \nu = 0 \end{array} \right\} , \tag{30c}$$

$$v(t,\tau) = \left\{ \begin{array}{ll} \frac{1}{|\tau|} G^*\left(\frac{t}{\tau}\right) & \text{for } \tau \neq 0 \\ \delta(t) & \text{for } \tau = 0 \end{array} \right\} , \tag{30d}$$

$$V(t,f) = 2 \, \mathrm{Re} \int_0^\infty \frac{dy}{y} \exp(i2\pi tfy) \, G\left(\frac{1}{y}\right) \; . \tag{30e}$$

This last result shows that the smoothing function $V(t,f)$ for a product kernel is always a function of the product tf, and is never a function of t or f separately.

The last integral on y converges at $y = 0$ if $G(\infty) = 0$. Alternatively, it converges at $y = 0$ for $G(\infty) \neq 0$ if $tf \neq 0$. And the integral converges at $y = \infty$ if $tf \neq 0$.

On the other hand, if $tf = 0$, then the last integral on y above is infinite if $G(0) \neq 0$; that is, $V(t,f) = \infty$ for $tf = 0$, which corresponds to both coordinate axes $t = 0$ and $f = 0$. The example in (25) is of this nature and corresponds to the special case of $g(x) = \exp(-x^2/\sigma^2)$ and $G(y) = \pi^{1/2}\sigma \exp(-\pi^2 y^2 \sigma^2)$, for which $G(0) = \pi^{1/2}\sigma \neq 0$.

DISCRETE-TIME CONSIDERATIONS

Up to this point, it has been assumed that $s(t)$ is available for continuous time t. Now, we address the case where the only knowledge of $s(t)$ is through samples taken at multiples of time increment Δ. The proper treatment of these samples $\{s(\kappa\Delta)\}$, in order to obtain an unaliased WDF $W(t,f)$, was determined in [2]; namely, it was found necessary to take $\Delta < 1/F$, where bandwidth F is specified in (3). Also, when an efficient FFT procedure for evaluating discrete spectral values of $S(f)$ was employed, it was found necessary to choose FFT size $N > 2T/\Delta$, where duration T is specified in (2). The following extension is aimed at obtaining an unaliased version of smoothed WDF $\mathbf{W}(t,f)$ defined in (19). The reader must be familiar with the procedures presented in [2].

EVALUATION OF MODIFIED CAF $\chi(\nu,\tau)$

As in [2; (69)], define

$$\overline{S}(f) = \left\{ \begin{array}{ll} \Delta \sum\limits_{k} \exp(-i2\pi f\Delta k)\, s(k\Delta) & \text{for } |f| < (2\Delta)^{-1} \\ 0 & \text{otherwise} \end{array} \right\} , \qquad (31)$$

where the sum on k is over all nonzero summand values. Then since $\Delta < 1/F$, we have $\overline{S}(f) = S(f)$ for all f; furthermore, $\overline{S}(f)$ can be computed at any f values of interest, directly from the available samples $\{s(k\Delta)\}$. Therefore, from (16), (7b), and (5), the modified continuous CAF is

$$\chi(\nu,\tau) = \tilde{v}(\nu,\tau) \int df \, \exp(i2\pi f\tau) \, \Phi(\nu,f) = \tag{32a}$$

$$= \tilde{v}(\nu,\tau) \int df \, \exp(i2\pi f\tau) \, \overline{S}(f+\tfrac{1}{2}\nu) \, \overline{S}^*(f-\tfrac{1}{2}\nu) \; . \tag{32b}$$

Now, in practice, $\overline{S}(f)$ must be computed at a discrete set of points; in particular, when we choose frequency increment $\Delta_f = 1/(N\Delta)$, where N is arbitrary, we obtain

$$\overline{S}\left(\frac{n}{N\Delta}\right) = \Delta \sum_k \exp(-i2\pi nk/N) \; s(k\Delta) \quad \text{for } |n| < \frac{N}{2} \; . \tag{33}$$

There is no need to consider n beyond the $\pm N/2$ range, because the argument f of $\overline{S}(f)$ then covers the $\pm 1/(2\Delta)$ frequency range, which is greater than the $\pm F/2$ range of $S(f)$ in (3). We adopt, as our approximation to desired function (32), the trapezoidal form

$$\chi_a(\nu,\tau) \equiv \tilde{v}(\nu,\tau) \, \frac{1}{N\Delta} \sum_j \exp\left(i2\pi\frac{j}{N\Delta}\tau\right) \overline{S}\left(\frac{j}{N\Delta} + \frac{\nu}{2}\right) \overline{S}^*\left(\frac{j}{N\Delta} - \frac{\nu}{2}\right)$$
$$\text{for all } \nu,\tau \; . \tag{34}$$

Now let infinite impulse train

$$\delta_b(x) \equiv \sum_k \delta(x - kb) \; . \tag{35}$$

Then, using $\Delta_f = 1/(N\Delta)$, (34) can be expressed and developed as

$$\chi_a(\nu,\tau) = \tilde{v}(\nu,\tau) \int df \, \exp(i2\pi f\tau) \, \Phi(\nu,f) \, \Delta_f \, \delta_{\Delta_f}(f) =$$

$$= \tilde{v}(\nu,\tau) \left[\chi(\nu,\tau) \overset{\tau}{\circledast} \sum_j \delta(\tau - jN\Delta)\right] =$$

$$= \tilde{v}(\nu,\tau) \sum_j \chi(\nu,\tau - jN\Delta) \quad \text{for all } \nu,\tau \; . \tag{36}$$

The sum on j in (36) represents sets of aliasing lobes spaced by multiples of $N\Delta$ on the τ axis. From figure 1, since the τ extent of $\chi(\nu,\tau)$ is $\pm T$, the first aliasing lobe in (36) for $j = 1$ extends down to $\tau = N\Delta - T$. In order that this lobe not overlap the desired main lobe, $j = 0$, we must have $T < N\Delta - T$, or

$$N > \frac{2T}{\Delta}\,, \qquad \Delta_f = \frac{1}{N\Delta} < \frac{1}{2T}\,. \tag{37}$$

This last constraint on Δ_f is consistent with the fact that the τ extents of $R(t,\tau)$ and $\chi(\nu,\tau)$ are $\pm T$; see figure 1 and [2; page A-4].

Equation (37) states that the size of the FFT in (33) must be at least equal to twice the number of waveform samples taken at increment Δ in duration T of s(t). When this selection is made, (36) and (16) yield

$$\chi_a(\nu,\tau) = \tilde{v}(\nu,\tau)\,\chi(\nu,\tau) = \chi(\nu,\tau) \quad \text{for } |\tau| < N\Delta/2\,, \quad \text{all } \nu\,. \tag{38}$$

That is, approximate GTFR $\chi_a(\nu,\tau)$, defined by the sum in (34), is equal to the desired GTFR $\chi(\nu,\tau)$ within a strip in the ν,τ plane.

Now, in order to convert (34) to a form where we can use the spectrum calculations (33), we limit ν to the values $2n/(N\Delta)$:

$$\chi\left(\frac{2n}{N\Delta},\tau\right) = \tilde{v}\left(\frac{2n}{N\Delta},\tau\right) \frac{1}{N\Delta} \sum_j \exp\left(i2\pi\frac{j}{N\Delta}\tau\right) \overline{S}\left(\frac{j+n}{N\Delta}\right) \overline{S}^*\left(\frac{j-n}{N\Delta}\right)$$

$$\text{for } |\tau| < \frac{N\Delta}{2}\,, \quad \text{all } n\,. \tag{39}$$

We have dropped the subscript a on $\chi(\nu,\tau)$, by virtue of (38). The ν increment in (39) is $\Delta_\nu = 2/(N\Delta)$, which is less than $1/T$

according to (37); this increment is fine enough to track variations of $\chi(\nu,\tau)$ in ν, since the t extent of the TFRs in figure 2 is $\pm T/2$.

Finally, in order to manipulate (39) into an FFT form, we restrict the τ-value calculations to the set

$$\chi\left(\frac{2n}{N\Delta}, m\Delta\right) = \tilde{v}\left(\frac{2n}{N\Delta}, m\Delta\right) \frac{1}{N\Delta} \sum_j \exp(i2\pi jm/N)\ \overline{S}\left(\frac{j+n}{N\Delta}\right)\ \overline{S}^*\left(\frac{j-n}{N\Delta}\right)$$

$$\text{for } |m| < \frac{N}{2}\ ,\quad \text{all } n\ . \qquad (40)$$

Actually, since the $|\nu|$ extent of $\chi(\nu,\tau)$ is $\min\{F,B/q\}$ according to (24), we only need to consider

$$\frac{2|n|}{N\Delta} < \min\{F,B/q\}\ , \quad \text{that is,}\ |n| < \frac{N}{2} \min\{F\Delta,B\Delta/q\}\ . \qquad (41)$$

But since we always have $F\Delta < 1$, then $|n| < N/2$ will always suffice. Thus, m and n in (40) can be limited to $\pm N/2$. The τ increment in (40) is $\Delta_\tau = \Delta < 1/F$, which is consistent with the fact that the f extents of $\Phi(\nu,f)$ and $W(t,f)$ are $\pm F/2$; see figure 1 and [2; page A-4].

We have shown here that if $\Delta < 1/F$ and $N > 2T/\Delta$, then an unaliased version of GTFR $\chi(\nu,\tau)$ is available and that this version can be efficiently computed by (40). These conditions are the same as those derived in [2; appendix D]. The multiplication of $\chi(\nu,\tau)$ by weighting $\tilde{v}(\nu,\tau)$ in (16) or (32) to obtain $\chi(\nu,\tau)$ has no effect on aliasing in the ν,τ plane; this is an obvious result in retrospect.

EVALUATION OF MODIFIED SCF $\Phi(\nu,f)$

The modified SCF $\Phi(\nu,f)$ is given by (17) as the Fourier transform of $\chi(\nu,\tau)$. Since $\chi(\nu,\tau)$ will only be available at increment $\Delta_\tau = \Delta$, as given by (40), we adopt as our approximation the trapezoidal form

$$\Phi_a(\nu,f) \equiv \Delta \sum_m \exp(-i2\pi f m\Delta)\ \chi(\nu,m\Delta) =$$

$$= \int d\tau\ \exp(-i2\pi f\tau)\ \chi(\nu,\tau)\ \Delta\ \delta_\Delta(\tau) =$$

$$= \Phi(\nu,f) \overset{f}{\circledast} \delta_{1/\Delta}(f) = \sum_m \Phi\left(\nu, f - \frac{m}{\Delta}\right) \quad \text{for all } \nu, f\ . \tag{42}$$

The first aliasing lobe for $m = 1$ is centered at $f = 1/\Delta$.

The f extent of GTFR $\Phi(\nu,f)$ is $\pm(\frac{1}{2}F + 1/D)$, as seen in figure 3. In order that aliasing be insignificant in (42), we must have $\frac{1}{2}F + 1/D < 1/(2\Delta)$; that is, time sampling increment Δ must satisfy the constraint

$$\Delta < \frac{1}{F + \frac{2}{D}}\ . \tag{43}$$

This is tighter than the original constraint $\Delta < 1/F$, which was sufficient for reconstruction of $s(t)$ and the unmodified TFRs such as $\chi(\nu,\tau)$ and $W(t,f)$. So if we anticipate doing some smoothing of the TFRs, sampling with a time increment Δ satisfying (43) must be undertaken in order to avoid aliasing. In this case, we have

$$\Phi_a(\nu,f) = \Phi(\nu,f) \quad \text{for } |f| < 1/(2\Delta)\ ,\ \text{all } \nu\ . \tag{44}$$

As for the actual evaluation of GTFR $\Phi(\nu,\tau)$, we use (42) and (44) to get

$$\Phi\left(\nu,\frac{j}{N\Delta}\right) = \Delta \sum_m \exp(-i2\pi jm/N)\ \chi(\nu,m\Delta) \quad \text{for } |j| < \frac{N}{2}\text{, all } \nu\ . \tag{45}$$

Finally, in order to use the available quantities in (40), we restrict the calculation to the values

$$\Phi\left(\frac{2n}{N\Delta},\frac{j}{N\Delta}\right) = \Delta \sum_m \exp(-i2\pi jm/N)\ \chi\left(\frac{2n}{N\Delta},m\Delta\right)$$
$$\text{for } |n| < \frac{N}{2}\ ,\ |j| < \frac{N}{2}\ . \tag{46}$$

This procedure in (46) yields unaliased samples of the GTFR $\Phi(\nu,\tau)$ when (43) is satisfied. It utilizes FFT operations, applied to the GTFR $\chi(\nu,\tau)$, which is available by the FFT prescription in (40). The ranges of integers n and j in (46) are sufficient to cover the range $\pm 1/\Delta$ and $\pm 1/(2\Delta)$ in ν and f, respectively. But since $1/\Delta > F + 2/D$ by (43), the ranges $\pm(F + 2/D)$ and $\pm(F/2 + 1/D)$ in ν and f, respectively, are adequate to fully cover the extent of GTFR $\Phi(\nu,f)$; see figure 3. The increment $\Delta_f = 1/(N\Delta)$ in (46) is fine enough to track $\Phi(\nu,f)$ in f, since $1/(N\Delta) < 1/(2T)$ by (37), while the τ extent of the GTFRs in figure 3 is always less than $\pm T$.

EVALUATION OF MODIFIED WDF $\mathbf{W}(t,f)$

The modified WDF $\mathbf{W}(t,f)$ was given by (19) as the Fourier transform of $\mathbf{R}(t,\tau)$. However, in analogy to the two alternatives in (6), there is also the form

$$\mathbf{W}(t,f) = \int d\nu \, \exp(i2\pi\nu t) \, \mathbf{\Phi}(\nu,f) \; . \tag{47}$$

Since $\mathbf{\Phi}(\nu,f)$ will only be available at increment $\Delta_\nu = 2/(N\Delta)$, as given by (46), we utilize the following trapezoidal approximation to (47):

$$\mathbf{W}_a(t,f) \equiv \frac{2}{N\Delta} \sum_n \exp\left(i2\pi\frac{2n}{N\Delta}t\right) \mathbf{\Phi}\left(\frac{2n}{N\Delta},f\right) =$$

$$= \int d\nu \, \exp(i2\pi\nu t) \, \mathbf{\Phi}(\nu,f) \, \Delta_\nu \, \delta_{\Delta_\nu}(\nu) =$$

$$= \mathbf{W}(t,f) \overset{t}{\circledast} \delta_{N\Delta/2}(t) = \sum_n \mathbf{W}\left(t - n\frac{N\Delta}{2},f\right) \quad \text{for all } t,f \; . \tag{48}$$

The first aliasing lobe for $n = 1$ is centered at $t = N\Delta/2$.

The t extent of GTFR $\mathbf{W}(t,f)$ is $\pm(\frac{1}{2}T + 1/B)$, as seen in figure 3. In order that aliasing be insignificant in (48), we must have $\frac{1}{2}T + 1/B < N\Delta/4$; that is, the FFT size N must satisfy

$$N > \frac{2T}{\Delta} + \frac{4}{B\Delta} \; . \tag{49}$$

This is more stringent than original constraint (37), which sufficed for the unmodified TFRs. Again, an unaliased smoothed WDF can only be achieved if sampling increment Δ is smaller and if the FFT size N is larger, the exact amounts depending on the degree of smoothing desired; see figure 2 in this regard. When (49) is satisfied, we have

$$\mathbf{W}_a(t,f) = \mathbf{W}(t,f) \quad \text{for } |t| < N\Delta/4 \text{ , all } f \text{ .} \tag{50}$$

The combination of (50), (48), and (46) now yields

$$\mathbf{W}\left(t,\frac{j}{N\Delta}\right) = \frac{2}{N\Delta} \sum_n \exp\left(i2\pi\frac{2n}{N\Delta}t\right) \mathbf{\Phi}\left(\frac{2n}{N\Delta},\frac{j}{N\Delta}\right)$$

$$\text{for } |t| < \frac{N\Delta}{4} \text{ , } \quad |j| < \frac{N}{2} \text{ .} \tag{51}$$

Finally, to convert (51) to an FFT, we restrict the t values to

$$\mathbf{W}\left(\frac{m\Delta}{2},\frac{j}{N\Delta}\right) = \frac{2}{N\Delta} \sum_n \exp(i2\pi nm/N) \ \mathbf{\Phi}\left(\frac{2n}{N\Delta},\frac{j}{N\Delta}\right)$$

$$\text{for } |m| < \frac{N}{2} \text{ , } \quad |j| < \frac{N}{2} \text{ .} \tag{52}$$

Again, N-point FFTs will realize the desired unaliased smoothed WDF $\mathbf{W}(t,f)$ at selected points that cover its full extent, with time and frequency increments that track the fastest possible variations of this function. In particular, (52) yields $\Delta_t = \Delta/2 < 1/(2F)$ and $\Delta_f = 1/(N\Delta) < 1/(2T)$. But since the ν extent of $\mathbf{\Phi}(\nu,f)$ in figure 3 is never larger than $\pm F$, while the τ extent of $R(t,\tau)$ is never larger than $\pm T$, these increments are certainly fine enough to track the variations; also see [2; appendix A]. The ranges of integers m and j in (52) cover interval $\pm N\Delta/4$ in t and bandwidth $\pm 1/(2\Delta)$ in f. But since $N\Delta/4 > T/2 + 1/B$ and $1/(2\Delta) > F/2 + 1/D$ according to (49) and (43), respectively, these t and f ranges cover the full extent of smoothed WDF $\mathbf{W}(t,f)$ in figure 3.

SUMMARY

Calculation of the modified CAF $\chi(\nu,\tau)$ can be done without changing the requirements on sampling increment Δ and FFT size N. However, in order to compute the modified SCF $\Phi(\nu,f)$, the sampling increment Δ must be taken at a smaller value, in order to avoid aliasing in frequency f. Finally, in order to compute the modified WDF $\mathbf{W}(t,f)$, both the sampling increment Δ must be smaller and the FFT size N must be larger, in order to avoid aliasing in time t and frequency f. If there is interest in calculation of the modified TCF $\mathbf{R}(t,\tau)$, it can be shown that aliasing will be controlled when FFT size N satisfies (49); the constraint (43) on Δ need not be met, insofar as calculation of $\mathbf{R}(t,\tau)$ is concerned, although we still need $\Delta < 1/F$. It is only when the final transformation into the t,f plane is accomplished that both constraints (43) and (49) must be met.

If integrals of products of WDFs or CAFs are of interest [6], the rules on sampling rate and FFT size given here should suffice to get accurate numerical results. The aliasing lobes have been kept out of the regions of interest, thereby minimizing possible interference effects.

A summary of the operations that must be undertaken on available time data samples $\{s(k\Delta)\}$ follows: compute the spectral quantities $\overline{S}$ in (33); use these in (40) to get samples of the weighted CAF χ; employ (46) to evaluate the modified SCF Φ; and use (52) to determine the smoothed WDF $\mathbf{W}$. All of these expressions use N-point FFTs.

Since the number of substantial samples of s(t) is T/Δ according to (2), the FFT size N in (33) is at least twice this large; see (37) and (49). Thus, approximately half of the N array locations input to (33) will contain rather small contributions. If s(t) is sampled well beyond $t = \pm T/2$, say for $|t| > T$, these very small values can be "collapsed" into the available N bins with no loss of accuracy; see [2; page 5].

Candidates for weighting $\tilde{v}(\nu,\tau)$ to be used in (40) include (12) or (20) or (25). The values of parameters B, D, r, and σ will have to be made by inspection of CAF $\chi(\nu,\tau)$, which is the factor multiplying $\tilde{v}(\nu,\tau)$ in (40). A check should then be made of (43) and (49) to ensure that aliasing is not significant.

REFERENCES

[1] L. Cohen, "Time-Frequency Distributions - A Review", **Proceedings of the IEEE**, volume 77, number 7, pages 941 - 981, July 1989.

[2] A. H. Nuttall, **Alias-Free Wigner Distribution Function and Complex Ambiguity Function for Discrete-Time Samples**, NUSC Technical Report 8533, Naval Underwater Systems Center, New London, CT, 14 April 1989.

[3] B. Harms, "Computing Time-Frequency Distributions", **IEEE Transactions on Acoustics, Speech, and Signal Processing**, accepted for publication, October 1990.

[4] A. H. Nuttall, **Wigner Distribution Function: Relation to Short-Term Spectral Estimation, Smoothing, and Performance in Noise**, NUSC Technical Report 8225, Naval Underwater Systems Center, New London, CT, 16 February 1988.

[5] H. I. Choi and W. J. Williams, "Improved Time-Frequency Representation of Multicomponent Signals using Exponential Kernels", **IEEE Transactions on Acoustics, Speech, and Signal Processing**, volume ASSP-37, number 6, pages 862 - 871, June 1989.

[6] A. H. Nuttall, **Two-Dimensional Convolutions, Correlations, and Fourier Transforms of Combinations of Wigner Distribution Functions and Complex Ambiguity Functions**, NUSC Technical Report 8759, Naval Underwater Systems Center, New London, CT, 6 August 1990.

INITIAL DISTRIBUTION LIST

Addressee	No. of Copies
Admiralty Underwater Weapons Establishment, England	
Library	1
Center for Naval Analyses	1
Coast Guard Academy	
Prof. J. J. Wolcin	1
David Taylor Research Center, Bethesda, MD	
Commander	1
H. Chaplin	1
L. Becker	1
W. Phillips (Code 1932)	1
David Taylor Research Center, Annapolis	
P. Prendergast (Code 2744)	1
Defense Nuclear Agency, RAAE	
J. Meyers	1
Defence Research Center, Australia	
Library	1
Defence Research Establishment Atlantic, Nova Scotia	
B. E. Mackey (Library)	1
Defence Research Establishment Pacific, British Columbia	
Dr. D. J. Thomson	1
Defence Science Establishment, HMNZ Dockyard, New Zealand	
Director	1
Defence Scientific Establishment, New Zealand	
Dr. L. H. Hall	1
Defense Advanced Research Projects Agency	
Commanding Officer	1
A. W. Ellinthorpe	1
Defense Intelligence Agency	1
Defense Technical Information Center	12
Dept. of Science & Industrial Research, New Zealand	
M. A. Poletti	1
National Radio Astronomy Observatory	
F. Schwab	1
National Security Agency	
Dr. J. R. Maar (R51)	1
Naval Air Development Center	
Commander	1
A. Witt	1
T. Madera	1
Naval Air Systems Command	
NAIR 93	1
Naval Coastal Systems Center	
Commanding Officer	1
D. Skinner	1
E. Linsenmeyer	1
Naval Environmental Prediction Research Facility	1
Naval Intelligence Command	1
Naval Oceanographic Office	1

INITIAL DISTRIBUTION LIST (CONT'D)

Addressee	No. of Copies
Naval Oceanographic & Atmospheric Research Laboratory, CA	
M. J. Pastore	1
Naval Oceanographic & Atmospheric Research Laboratory, MS	
Commanding Officer	1
R. Wagstaff (Code 245)	1
B. Adams	1
E. Franchi	1
R. Fiddler (Code 245)	1
Naval Ocean Systems Center, Hawaii	1
Naval Ocean Systems Center, San Diego	
Commanding Officer	1
J. M. Alsup (Code 635)	1
J. Silva	1
D. Hanna	1
P. Nachtigall	1
W. Marsh	1
Naval Personnel Research & Development Center	1
Naval Postgraduate School	
Superintendent	2
Prof. C. W. Therrien (Code 62 TI)	1
Naval Research Laboratory, Orlando, USRD	1
Naval Research Laboratory, Washington	
Commanding Officer	1
Dr. P. B. Abraham (Code 5131)	1
W. F. Gabriel (Code 5370)	1
A. A. Gerlach	1
N. Yen (Code 5130)	1
D. Bradley	1
S. Sachs	1
S. Wolfe	1
D. Steiger	1
Naval Sea Systems Command	
SEA-00; -63; 63D; -63X; -92R; PMS-402	6
Naval Surface Warfare Center	
J. Gray (Code G71)	1
Naval Surface Weapons Center, Dahlgren, VA	
Commander	1
H. Crisp	1
D. Phillips	1
T. Ryczek	1
Naval Surface Weapons Center, White Oak Lab.	1
Naval Surface Weapons Center, Fort Lauderdale	1
Naval Technical Intelligence Center	
Commanding Officer	2
D. Rothenberger	1
Naval Underwater Systems Center, West Palm Beach	
Officer in Charge	1
Dr. R. M. Kennedy (Code 3802)	1

INITIAL DISTRIBUTION LIST (CONT'D)

Addressee	No. of Copies
Naval Weapons Center	1
Norwegian Defence Research Establishment	
Dr. J. Glattetre	1
Office of the Chief of Naval Research, Arlington, VA	
OCNR 00; -10; -11; -12; -13; -20; -21; -22; -23 (3)	11
N. L. Gerr (Code 1111)	1
A. Wood	1
D. Johnson	1
SACLANT Undersea Research Center	
Dr. J. P. Ianniello	1
Dr. S. Stergiopolous	1
Prof. G. Tacconi	1
Library	1
Sonar and Surveillance Group, RANRL, Australia	1
Space & Naval Warfare System Command	
SPAWAR-00; -04; -005; PD-80; PMW-181	5
L. Parrish	1
U.S. Air Force, Alabama	
Air University Library	1
U.S. Coast Guard Research & Development Center	
Library	1
U.S. Department of Commerce, NTIA/ITS	
Dr. A. D. Spaulding	1
Weapons Systems Research Laboratory, Australia	
HASC	1
HSPC	1
Brown University	
Documents Library	1
Canberra College of Advanced Education	
P. Morgan	1
Concordia University, Quebec	
Prof. J. Krolik	1
Dalhousie University	
Dr. B. Ruddick	1
Drexel University	
Prof. S. B. Kesler	1
Harvard University	
Gordon McKay Library	1
Indian Institute of Technology, India	
Dr. K. M. M. Prabhu	1
Johns Hopkins University, Applied Physics Laboratory	
Director	1
J. C. Stapleton	1
Kansas State University	
Prof. B. Harms	1
Lawrence Livermore National Laboratory	
Director	1
L. C. Ng	1

INITIAL DISTRIBUTION LIST (CONT'D)

Addressee	No. of Copies
Los Alamos National Laboratory	1
Marine Biological Laboratory, Woods Hole	1
Marine Physical Laboratory, Scripps	1
Massachusetts Institute of Technology	
Prof. A. B. Baggaroer	1
Barker Engineering Library	1
Northeastern University	
Prof. C. L. Nikias	1
Penn State University, Applied Research Laboratory	
Director	1
F. W. Symons	1
R. Hettche	1
E. Liszka	1
Purdue University	
Prof. N. Srinivasa	1
Royal Military College of Canada	
Prof. Y. T. Chan	1
Rutgers University	
Prof. S. Orfanidis	1
San Diego State University	
Prof. F. J. Harris	1
Sandia National Laboratory	
Director	1
J. Claasen (315)	1
Simon Fraser University	
Dr. E. F. Velez	1
Southeastern Massachusetts University	
Prof. C. H. Chen	1
State University of New York	
Prof. M. Barkat	1
Tel Aviv University, Israel	
Prof. E. Weinstein	1
United Engineering Center	
Engineering Societies Library	1
University of Alberta, Canada	
K. L. Yeung	1
University of Auckland	
Dr. M. D. Johns	1
University of California, San Diego	
Prof. C. W. Helstrom	1
University of Colorado	
Prof. L. L. Scharf	1
University of Connecticut	
Prof. C. H. Knapp	1
Wilbur Cross Library	1
University of Florida	
Prof. D. C. Childers	1
University of Illinois	
Dr. D. L. Jones	1

INITIAL DISTRIBUTION LIST (CONT'D)

Addressee	No. of Copies
University of Michigan	
Communications & Signal Processing Laboratory	1
W. J. Williams	1
University of Minnesota	
Prof. M. Kaveh	1
University of Queensland	
Dr. B. Boashash	1
University of Rhode Island	
Prof. G. F. Boudreaux Bartels	1
Prof. S. M. Kay	1
Prof. D. Tufts	1
Library	1
University of Rochester	
Prof. E. Titlebaum	1
University of Southern California	
Prof. W. C. Lindsey	1
Dr. A. Polydoros	1
University of Strathclyde, Scotland	
Prof. T. S. Durrani	1
University of Technology, England	
Prof. J. W. R. Griffiths	1
University of Texas, Applied Research Laboratory	1
University of Washington	
Applied Physics Laboratory	1
Prof. D. W. Lytle	1
Dr. R. C. Spindel	1
Villanova University	
Prof. M. G. Amin	1
Woods Hole Oceanographic Institution	
Director	1
Dr. E. Weinstein	1
Yale University	
Prof. A. Nehorai	1
Prof. P. M. Schultheiss	1
Prof. F. Tuteur	1
Kline Science Library	1
Applied Seismic Group	
R. Lacoss	1
A&T, North Stonington, CT	
H. Jarvis	1
A&T, Arlington, VA	
D. L. Clark	1
BB&N, Arlington, VA	
Dr. H. Cox	1
BB&N, Cambridge, MA	
H. Gish	1
BB&N, New London, CT	
Dr. P. G. Cable	1

INITIAL DISTRIBUTION LIST (CONT'D)

Addressee	No. of Copies
Bell Communications Research	
J. F. Kaiser	1
D. Sunday	1
Cogent Systems, Inc.	
J. P. Costas	1
Diagnostic/Retrieval Systems, Inc.	
J. Williams	1
EDO Corporation	
M. Blanchard	1
EG&G	
D. Frohman	1
General Electric Company, Moorestown, NJ	
Dr. M. R. Allen	1
H. Urkowitz	1
General Electric Company, Philadelphia, PA	
T. J. McFall	1
General Electric Company, Pittsfield, MA	
R. W. Race	1
General Electric Company, Syracuse, NY	
Dr. A. M. Vural	1
D. Winfield	1
Harris Scientific Services	
B. Harris	1
Hughes Aircraft Company, Buena Park, CA	
T. E. Posch	1
IBM	
G. L. Demuth	1
Interstate Electronics Corporation	
R. O. Nielsen (Dept. 8011)	1
Kildare Corporation	
Dr. R. Mellen	1
Lincom Corporation	
Dr. T. A. Schonhoff	1
Magnavox Elec. Systems Company	
R. Kenefic (Dept. 525)	1
MSB Systems, Inc.	
A. Winder	1
Nichols Research Corporation	
Dr. T. L. Marzetta	1
Orincon Corporation	
S. L. Marple	1
Dr. J. W. Young	1
Prometheus, Inc., Newport, RI	
M. J. Barrett	1
Prometheus, Inc., Sharon, MA	
Dr. J. S. Byrnes	1
RAN Research Lab, Australia	1

INITIAL DISTRIBUTION LIST (CONT'D)

Addressee	No. of Copies
Raytheon, Portsmouth, RI	
J. Bartram	1
R. Conner	1
S. S. Reese	1
Rockwell International	
L. T. Einstein	1
Dr. D. F. Elliott	1
SAIC, Falls Church, VA	
Dr. P. Mikhalevsky	1
SAIC, New London	
Dr. F. DiNapoli	1
SIMRAD SUBSEA A/S, Naval Systems Div.	
E. B. Lunde	1
Sperry Corporation, Defense Marine Systems Unit	1
Toyon Research Corporation	
M. L. Van Blaricum	1
Tracor	
Dr. T. J. Leih	1
TRW, Fairfax, VA	
R. Prager	1
G. Maher	1
TRW, New London, CT	
D. Sturim	1
Welse Sistemi Subacquei, Genova, Italy	
Dr. H. Van Asselt	1
Westinghouse Electric Corporation, Annapolis, MD	
H. Newman	1
Dr. H. L. Price	1
Westinghouse Electric Corporation, Baltimore, MD	
R. Park	1
Westinghouse Electric Corporation, Waltham, MA	
R. B. Kennedy	1
Assard, G. L.	1
Beidas, B.	1
Bendat, Dr. J. S.	1
Bleistein, Dr. N.	1
Cohen, Dr. L.	1
Hahn, W. R.	1
Lloyd, L.	1
Maltz, F.	1
Middleton, Dr. D.	1
Nash, H. E.	1
Nicholson, D.	1
O'Brien, W.	1
Papoutsanis, P.D.	1
Pohler, R. F.	1

INITIAL DISTRIBUTION LIST (CONT'D)

Addressee	No. of Copies
Price, Dr. R.	1
Raisbeck, Dr. G.	1
Richter, W.	1
Schulkin, Dr. M.	1
Urick, R. J.	1
Von Winkle, Dr. W. A.	1
Werbner, A.	1
Wilson, Dr. J. H.	1